Preparation of quaternary solution processed chalcogenide thin films using mixtures of separate $As_{40}S_{60}$ and $Ge_{20}Sb_5S_{75}$ glass solutions

Jiri Jancalek [1], Stanislav Slang[1], Michal Kurka[1], Karel Palka[1, 2*], Miroslav Vlcek[1]

[1] Center of Materials and Nanotechnologies, Faculty of Chemical Technology, University of Pardubice, Studentska 95, 53210 Pardubice, Czech Republic
[2] Department of General and Inorganic Chemistry, Faculty of Chemical Technology, University of Pardubice, Studentska 95, 53210 Pardubice, Czech Republic

*karel.palka@upce.cz

Keywords
Chalcogenide, Thin films, Spin-coating, Solution mixture

Highlights

- Quaternary spin-coated thin films with specular optical quality were prepared.
- Separately dissolved $As_{40}S_{60}$ and $Ge_{20}Sb_5S_{75}$ were mixed for film composition tuning.
- Compositional, structural, optical properties and chemical resistance were studied.
- Linear dependence of physico-chemical properties on films composition observed.

Abstract
In this work, the chalcogenide glass thin films of As-Ge-Sb-S system were prepared in specular optical quality by spin-coating from mixtures of separate $As_{40}S_{60}$ and $Ge_{20}Sb_5S_{75}$ glass solutions. The five compositions were studied in total (0, 25, 50, 75 and 100 at.% of $As_{40}S_{60}$) to examine the possibility of deposition of quaternary chalcogenide glass thin films from mixture of simpler compositions solutions. The composition, organic residual content, structure, thickness, surface roughness, optical properties and chemical resistance of prepared films were studied in dependence on annealing temperature (up to 180 °C) and targeted composition. Thermally induced structural changes resulted in thin films with high optical quality and chemically stable polymerized glass structure. Physico-chemical properties of prepared mixed compositions thin films showed nearly linear combination of properties observed on $As_{40}S_{60}$ and $Ge_{20}Sb_5S_{75}$ thin films.

1. Introduction

Chalcogenide glasses are interesting optical materials, which have been studied for several decades for their wide IR transparency region, high refractive index and frequent sensitivity to various kinds of radiation [1-3]. Chalcogenide glasses can be used as a bulk material (e.g. windows or lenses for IR optics [4,5]) or as thin film on appropriate substrate (e.g. planar waveguides, high resolution photo- and/or e^- beam resists, phase change memories media [6-8]). Chalcogenide thin films can be deposited from their solution in organic bases, using techniques such as spin-coating, spiral bar-coating, electrospray, inkjet printing [9-12], or from gaseous phase by thermal vapour deposition, sputtering, laser ablation or chemical vapour deposition [13,14,15].

Solution deposition route exploits solubility of chalcogenide glasses in alkaline solvents, mainly in aliphatic amines. One of the major advantage of solution deposition route is the possibility to integrate different substances or materials to the glass solution or co-dissolution of chalcogenide glass and dopant material. Deposited thin films may have significantly modified physico-chemical

properties [16,17] or some new additional properties can be introduced (e.g. photoluminescence or photoconductivity [18-21]).

This study investigates the possibility of using mixtures of two separately dissolved chalcogenide glasses ($As_{40}S_{60}$ and $Ge_{20}Sb_5S_{75}$) for preparation of thin films in optical quality. The chalcogenide glasses were chosen due to the significant differences in their refractive index *n* and optical band gap E_g^{opt} [22-24]. Moreover, the $As_{40}S_{60}$ bulk glass and thin films were already thoroughly studied and bulk glass is commercially available as AMTIR 6, IRG 27 or IRRADIANCE™ Classic-1. The annealed $Ge_{20}Sb_5S_{75}$ solution processed thin films showed very high chemical stability that allows thickness tuning using layer stacking [25] and proved to be suitable for preparation of solution processed thin films with high optical quality. In this paper, we show the influence of composition and thermal post-deposition treatment on structure, thickness, surface roughness, organic residual content, optical properties and chemical resistance of spin-coated thin films prepared by mixing of two different glass solutions.

2. Experimental details

The source chalcogenide glass bulks of $As_{40}S_{60}$ and $Ge_{20}Sb_5S_{75}$ compositions were prepared using standard melt-quenching method. Quartz ampules were cleaned using aqua regia to remove organic and inorganic impurities then rinsed with redistilled water and dried. Appropriate quantities of high purity 5N elements were weighted into cleaned ampules and subsequently the ampules were evacuated (~ 10^{-3} Pa) and sealed. The synthesis were performed in rocking tube furnace at 800 °C for 32 hours for $As_{40}S_{60}$ bulk glass and at 950 °C for 72 hours for $Ge_{20}Sb_5S_{75}$ glass. The quartz ampules with melted glass were quenched in cold water.

Both source bulk glasses were powdered in agate bowl and separately dissolved in n-butylamine (BA) with concentration of 0.075 g of glass powder per 1 ml of BA solvent. After complete dissolution of chalcogenide glasses the solutions were mixed in corresponding quantities to reach required compositions of mixed thin films $(As_{40}S_{60})_x(Ge_{20}Sb_5S_{75})_{100-x}$, where x = 0, 25, 50, 75 and 100. All Prepared chalcogenide glass solutions and their mixtures were clear without any precipitate or turbidity.

Chalcogenide glass thin films were deposited onto soda lime square 2.5 x 2.5 cm substrates by spin-coating (SC) technique (spin-coater SC110, Best Tolls) in argon atmosphere at 3000 rpm for 120 s. Immediately after deposition the thin films were stabilized on a hot plate (HP-20D hotplate, Witeg) by annealing at 60 °C for 20 minutes (hereafter referred as as-prepared thin films). As-prepared thin films were annealed at 100, 140 and 180 °C for 60 minutes in argon filled chamber. The highest annealing temperature was chosen with respect to the T_g of $As_{40}S_{60}$ chalcogenide glass (~ 184 °C [26]).

Compositions of prepared thin films were investigated using energy dispersive X-ray analysis (EDS) by Aztec X-Max 20 detector (Oxford Instruments) installed in scanning electron microscope LYRA 3 (Tescan). The analysis were performed using 5 kV acceleration voltage. Samples were measured at four 400 × 400 μm areas and obtained compositions were averaged. Error bars represent standard deviation of measured values.

Structure of prepared thin films were studied by Raman spectroscopy using MultiRAM (Bruker) FT-Raman spectrometer equipped by 1064 nm Nd:YAG laser. Measurement were performed using excitation beam intensities of 55 mW with resolution of 2 cm^{-1} and averaging of 64 scans. Presented Raman spectra were normalized by the intensity of the band at 344 cm^{-1}. Due to the high luminescence, no measurements of the spin-coated thin films annealed at 180 °C were performed.

The transmission spectra of thin films were measured using UV-VIS-NIR spectrometer UV3600 (Shimadzu) in spectral range 190 – 2000 nm. The thicknesses and refractive index values of thin films were determined using evaluation method described in [27] based on Wemple-DiDomenico's parametrization of spectral dependence of refractive index [28] and the model of thin film transmission spectra presented by R. Swanepoel [29]. Presented data of thickness and refraction index represent average values obtained by measurement and evaluation of six samples of each treatment. Error bars represent standard deviation of obtained values.

Measurement of thin film roughness were performed using Solver Next (NT-MDT) atomic force microscope equipped with NSG10 tips (NT-MDT). Surface roughness of thin films was determined from the AFM scans measured at four 5 × 5 μm areas on samples of each treatment as root mean square value (RMS) according to ISO 4287/1 norm. Error bars represent standard deviation of calculated values.

Prepared thin films were etched in solution of 5 vol. % BA in dimethylsulfoxide at 25 °C. Etching rates were evaluated using procedure described in [30].

3. Results and discussion

Composition of prepared spin-coated thin films was analysed by EDS. Experimental data (figure 1) showed minor deviations from the targeted compositions. The results show that the most significant composition deviation are in sulfur and arsenic content. Depletion in arsenic content (up to ~ 4 at. % in case of $As_{40}S_{60}$ thin films) can be caused by partial oxidation of thin films during storage and transport of samples at ambient conditions, which subsequently leads to evaporation of arsenic oxides in SEM vacuum chamber. Similar observation of arsenic depletion in solution processed thin films were observed in our previous results in [31]. Sulfur deficiency in annealed $Ge_{20}Sb_5S_{75}$ thin films is probably caused by partial evaporation of non-bonded sulfur during high temperature annealing due to the significant sulfur overstoichiometry. With increasing content of $As_{40}S_{60}$ in mixed chalcogenide glass thin films the effect of thermally induced sulfur loss is less pronoun as the total sulfur overstoichimetry is gradually decreasing. The composition of mixed $(As_{40}S_{60})_x(Ge_{20}Sb_5S_{75})_{100-x}$ thin films are close to the targeted values (experimental error of EDS analysis ±1 at. %).

Fig. 1: The elemental composition of as-prepared and annealed (180 °C) solution processed $(As_{40}S_{60})_x(Ge_{20}Sb_5S_{75})_{100-x}$ thin films.

The total nitrogen content in thin films was also studied by EDS analysis. The BA molecule contains only one atom of nitrogen and no other nitrogen sources are expected due to the thin film deposition method applied. Thus, nitrogen content in thin film represents the residua of solvent molecules and their salts in thin film matrix. The nitrogen content in thin films (figure 2) of all studied compositions decreases monotonously with increasing annealing temperature. Significantly less steep decline of nitrogen content between 60 – 100 °C in case of $Ge_{20}Sb_5S_{75}$ and 25 % $As_{40}S_{60}$ thin films confirms the previous findings about different thermal stability of alkyl ammonium arsenic sulfide (AAAS) salts and alkyl ammonium germanium sulfide (AAGS) analogues. According [32] majority of AAAS salts decompose between 80 - 90 °C in comparison with AAGS salt which decompose at temperatures higher than 120 °C [33].

It is also evident from figure 2 that nitrogen content decreases with increasing content of $As_{40}S_{60}$. The higher nitrogen content (and thus content of organic residuals) in Ge-Sb-S based thin films can be explained by different size of glass dissolution products. According to [34] dissolution of Ge-Sb-S bulk glass leads to the nearly molecular sizes clusters. Contrary, dissolution of As-S bulk glasses results in significantly larger clusters with dimension of several nanometers [35,36). Lower size of glass clusters leads to higher solvation ratio that is subsequently reflected in a higher content of organic residues in thin films with higher $Ge_{20}Sb_5S_{75}$ content.

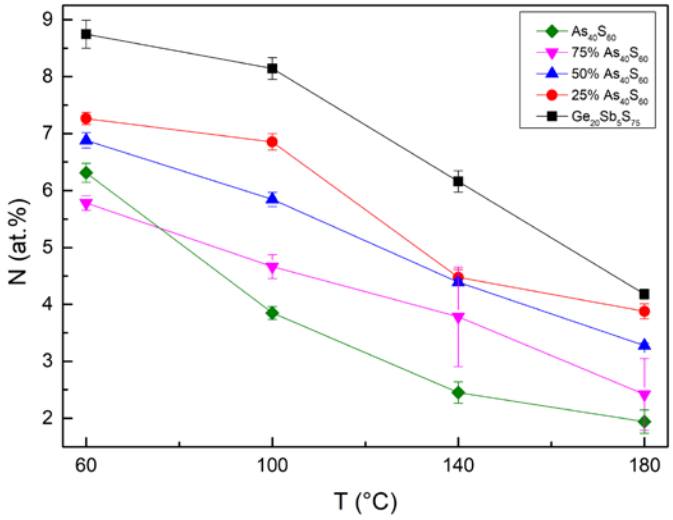

Fig. 2: Annealing temperature dependence of the nitrogen content in studied solution processed $(As_{40}S_{60})_x(Ge_{20}Sb_5S_{75})_{100-x}$ thin films.

The structure of deposited $(As_{40}S_{60})_x(Ge_{20}Sb_5S_{75})_{100-x}$ chalcogenide glasses thin films was determined by Raman spectroscopy. The Raman spectra of as-prepared thin films and thin films annealed at 100 and 140°C are present in figure 3. Measurements of thin films annealed at 180°C were not performed due to oversaturation of detector by luminescence signal even at lowest excitation laser power.

Fig. 3: Raman spectra of as-prepared and annealed solution processed thin films of source $As_{40}S_{60}$ and $Ge_{20}Sb_5S_{75}$ as well as mixed $(As_{40}S_{60})_x(Ge_{20}Sb_5S_{75})_{100-x}$ compositions.

The dominant band of as-prepared $As_{40}S_{60}$ thin films is situated at 369 cm^{-1} and corresponds to the vibrations of arsenic-rich realgar-like As_4S_4 units [37,38]. The presence of arsenic rich units in stoichiometric $As_{40}S_{60}$ thin films is compensated by content of S-S chains (490 cm^{-1}) or rings S_8 (475 cm^{-1}) [39, 40]. All of these structural units originated from chalcogenide glass dissolution process and they can be regularly found in as-prepared thin films of As-S system [40]. The distinctive shoulder around 345 cm^{-1} give evidence of presence of pyramidal polymer $AsS_{3/2}$ structural units [38,41,42]. The band at 420 cm^{-1} corresponds to the vibration of ionic alkyl ammonium arsenic sulfide (AAAS) salts [40,42,43]. The annealing process induces thermal decomposition of AAAS salts connected with release of organic residuals (as seen on EDS) and structural polymerization of chalcogenide glass matrix [43]. The bands of As_4S_4, S_8 ring and AAAS salts are decreasing while the band of $AsS_{3/2}$ pyramidal units is increasing.

The dominant band of as-prepared $Ge_{20}Sb_5S_{75}$ chalcogenide glass thin film is situated at 340 cm^{-1} and can be attributed to the vibrations of corner shared $GeS_{4/2}$ tetrahedral units [41,42]. Sharp shape of band is probably caused by high fragmentation and small size of molecular clusters (as discussed above). The main Raman band at 340 cm^{-1} is accompanied by wide band around 300 cm^{-1}, which corresponds to the vibrations of $SbS_{3/2}$ pyramidal units [22]. Significant overstoichiometry of sulfur in $Ge_{20}Sb_5S_{75}$ composition is manifested by presence of bands at 150, 219 and 475 cm^{-1} belonging to sulfur rings S_8 [39,40] and sulfur chains S-S at 490 cm^{-1} [39,40]. Three additional bands at 142, 190 and 455 cm^{-1} can be attributed to the vibrations of ionic dissolution products in form of AAGS salts [22,25,42]. Similarly to the $As_{40}S_{60}$ thin films, the annealing induces decomposition of AAGS salts and consequently structural polymerization. As the annealing temperature increases, the main band of corner shared $GeS_{4/2}$ tetrahedral units at 340 cm^{-1} is widening, band of edge-shared $GeS_{4/2}$ units at 368 cm^{-1} [44,45] starts to appear in measured spectra and intensities of bands of sulfur rings S_8 and AAGS salts are gradually decreasing. Based on results of thickness, optical properties and etching, presented below, we assume, that thermally induced structural changes are not completely finished

at 140 °C, but due to the strong luminescence of samples annealed at 180 °C we cannot provide Raman spectra with structure of fully stabilized thin films.

The Raman spectra of as-prepared thin films of mixed $(As_{40}S_{60})_x(Ge_{20}Sb_5S_{75})_{100-x}$ compositions show typical bands of both $As_{40}S_{60}$ and $Ge_{20}Sb_5S_{75}$ thin films. With increasing content of $As_{40}S_{60}$ in thin film composition, the sharp band of $GeS_{4/2}$ tetrahedral units at 340 cm^{-1} becoming less dominant and the wider bands of realgar-like As_4S_4 (369 cm^{-1}) and pyramidal $AsS_{3/2}$ (345 cm^{-1}) structural units appear. Decreasing total sulfur overstoichiometry is reflected in decreasing intensities of S_8 bands at 150, 219 and 475 cm^{-1}. Annealing induces structural polymerization of all present As-S, Ge-S and sulfur based structural units to the form of more compact material with less content of organic residuals.

Transmission of all studied samples were investigated in UV-VIS-NIR spectral region. Transmission spectra presented in figure 4 confirmed the high optical quality of the deposited thin films. Measured transmission spectra were evaluated by the procedure published in [27] to obtain refraction index at 1550 nm ($n_{1550\,nm}$) and thickness values (d).

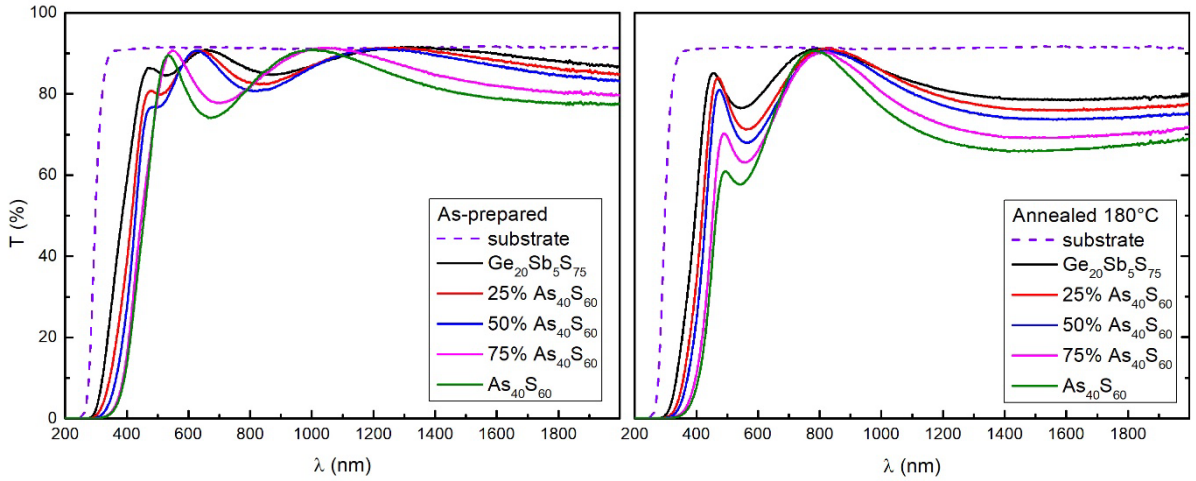

Fig. 4: Transmission spectra of solution processed as-prepared thin films (left) and thin films annealed at the highest temperature 180°C (right) .

Thickness d of all studied thin films decreases continuously with increasing content of $As_{40}S_{60}$ and increasing annealing temperature (figure 5 left) due to the decrease of organic residua content, which corresponds well to the findings from the EDS analysis and Raman spectroscopy. Higher amount of organic residuals in $Ge_{20}Sb_5S_{75}$ rich thin films is also reflected in higher thickness contraction, which decrease with increasing $As_{40}S_{60}$ content from ~ 45 % for $Ge_{20}Sb_5S_{75}$ thin films to ~36 % for $As_{40}S_{60}$ thin films (both annealed at 180 °C). High optical quality is maintained due to very low surface roughness of studied samples (figure 5 right), especially for samples annealed below 180 °C, where their surface roughness does not exceed 1 nm. In case of the samples annealed at highest temperature (180 °C), the surface roughness increases up to ~ 3.4 nm, but it is still too low to significantly influence optical quality of annealed thin films. Increase of thin film roughness is probably caused by both annealing induced structural changes given at temperatures close to the T_g of $As_{40}S_{60}$ glass composition (~ 184°C [26]) and observed volume contraction.

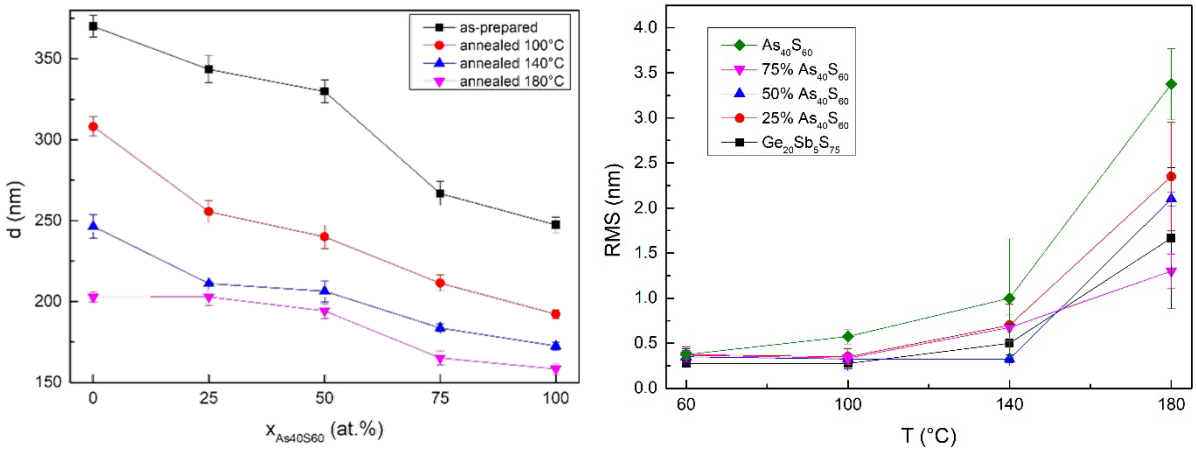

Fig. 5: Compositional dependence of the thickness (left) and annealing temperature dependence of surface roughness (right) of studied $(As_{40}S_{60})_x(Ge_{20}Sb_5S_{75})_{100-x}$ thin films.

AFM scans of as-prepared and the highest temperature annealed thin films showing the topography of the thin films surfaces are shown in figure 6.

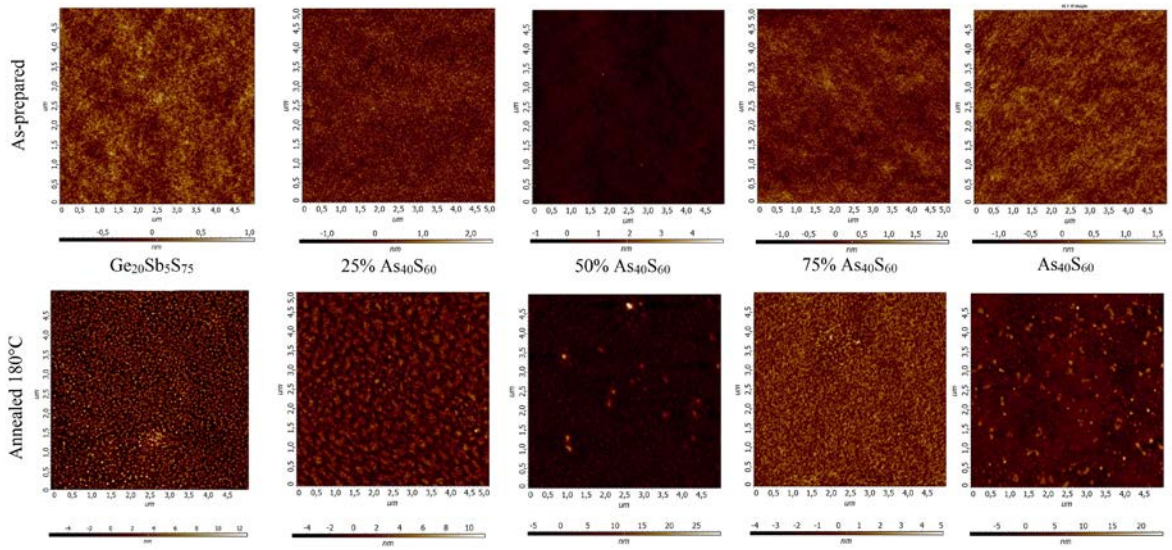

Fig. 6: AFM scans of as-prepared and annealed (180°C) thin films.

Refractive index at 1550 nm (n_{1550nm}) of solution processed thin films increases both with increasing annealing temperature and $As_{40}S_{60}$ content (figure 7). Significant increase of refractive index with annealing temperature is caused by release of the organic residuals and structural polymerization of the thin film matrix, which is in good agreement with conclusions from EDS and Raman spectroscopy and previously published results of similar systems [32,43]. Refractive index shows almost linear dependence on thin film composition.

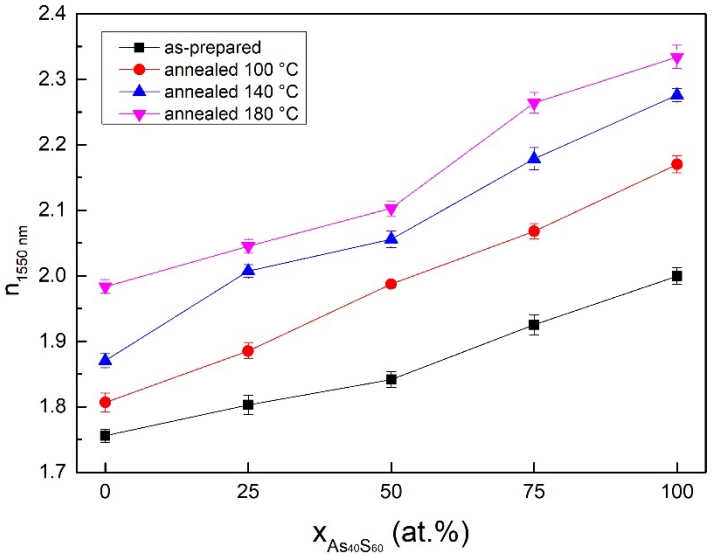

Fig. 7: Compositional dependence of refraction index at 1550 nm of studied $(As_{40}S_{60})_x(Ge_{20}Sb_5S_{75})_{100-x}$ thin films.

Due to the close position of shortwavelength absorption edge of the substrate and $Ge_{20}Sb_5S_{75}$ and 25 % $As_{40}S_{60}$ thin films, as it is apparent from figure 4, it is not possible to evaluate correctly optical band gap E_g^{opt} using standard Tauc´s method for semiconductors [46]. Darkening of thin film with increasing content of $As_{40}S_{60}$ is still obvious from position of shortwavelength absorption edge. Thus, the shortwavelength absorption edge is represent here by the wavelength at 5% of transmission (from measured transmission spectra). Figure 8 shows that absorption edge shifts to the longer wavelengths (red shift, darkening) with increasing content of $As_{40}S_{60}$. Similarly to the refractive index, values of wavelength at 5% transmission show almost linear dependence on thin films composition. The red shift (darkening) is also apparent with increasing annealing temperature. This suggests a decrease in the optical bandgap, which is in good agreement with previously observed results on spin-coated thin films of both As- and Ge-based chalcogenide glass systems [33, 47, 48]. Because both refraction index and position of the shortwave absorption edge exhibit a nearly linear increase with increasing content of $As_{40}S_{60}$, it is possible to use the layers prepared by mixing of $As_{40}S_{60}$ and $Ge_{20}Sb_5S_{75}$ solutions for preparation of suitable optical materials in specular optical quality and tailoring of their optical properties.

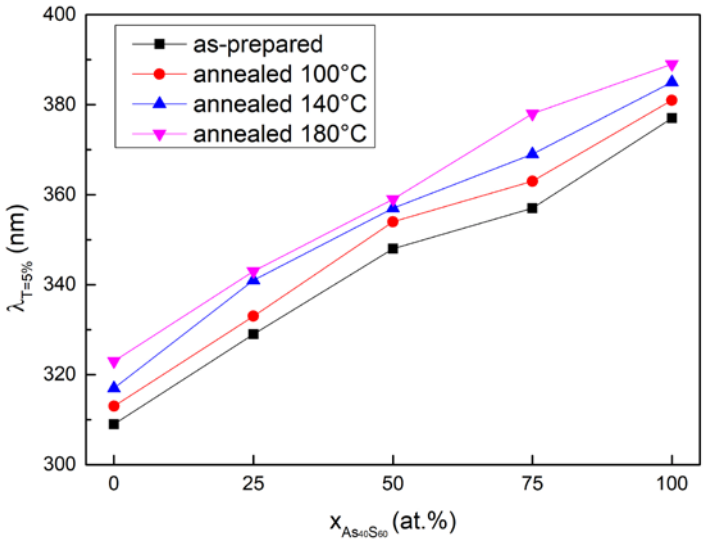

Fig. 8: Compositional dependence of shortwave absorption edge position (at 5 % of transmittance) of studied $(As_{40}S_{60})_x(Ge_{20}Sb_5S_{75})_{100-x}$ thin films.

The chemical resistance of thin films was investigated by measuring the etching kinetics in 5 vol. % n-butylamine in dimethylsulfoxide etching solution at 25°C. The etching rates were evaluated using procedure described in [30]. Obtained averaged values of etching rates are provided in figure 9. In case of as-prepared thin films the etching rates decrease sharply with increase of $As_{40}S_{60}$ content from ~ 210 nm·s^{-1} for $Ge_{20}Sb_5S_{75}$ thin film to ~ 40 nm·s^{-1} for $As_{40}S_{60}$ thin film. This significantly lower chemical resistance of as-prepared $Ge_{20}Sb_5S_{75}$ thin film can be explained by higher content of organic residuals and high fragmentation of the glass structure confirmed by sharpness of the main band in Raman spectrum (see Fig. 3). With increasing annealing temperature the chemical resistance of thin films also increases due to the thermally induced structural polymerization and release of organic residuals. In case of thin films annealed at 100 °C with 50, 75 and 100% of $As_{40}S_{60}$ similar chemical resistivity can be observed, because substantial part of organic residuals (in form of AAAS salts) are already decomposed between 80-90 °C. It results in more polymerized and chemically stable thin films in comparison with $Ge_{20}Sb_5S_{75}$ rich samples (0 and 25% of $As_{40}S_{60}$), where more dominant AAGS salts are decomposed at significantly higher temperatures (over 120 °C [33]). For all $As_{40}S_{60}$ containing thin films annealed at 180 °C the chemical resistance is almost identical. However, chemical resistance of $Ge_{20}Sb_5S_{75}$ glass thin films (0% $As_{40}S_{60}$) annealed at 180°C is still sharply increasing. This shows that even 25% addition of $As_{40}S_{60}$ significantly reduces chemical resistance of annealed $Ge_{20}Sb_5S_{75}$ thin films. It can be potentially explained by different reactivity of As-S and Ge-S structural units in both chalcogenide glasses ($As_{40}S_{60}$ and $Ge_{20}Sb_5S_{75}$). Based on dissolution mechanism proposed by Chern and Lauks [49], the arsenic with non-bonding electron pair offers another center for nucleophilic substitution which probably fastens whole dissolution process. We can also speculate that the significantly smaller sizes of $Ge_{20}Sb_5S_{75}$ glass dissolution products also significantly decrease the dissolution rate of studied samples. Obtained results of high chemical resistance of annealed $Ge_{20}Sb_5S_{75}$ are in a good agreement with our previous studies on Ge-Sb-S thin films [22,25].

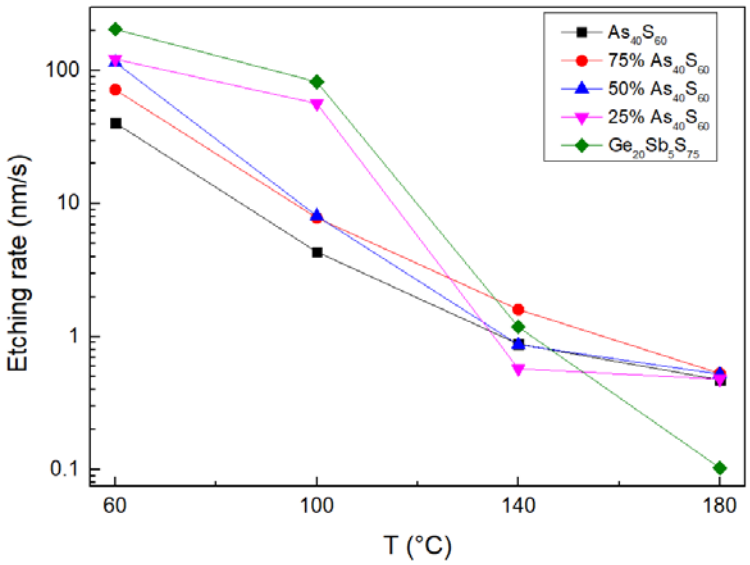

Fig. 9: Annealing temperature dependence of thin films etching rates in 5 vol. % BA in dimethylsulfoxide etching bath.

4. Conclusions

In presented work we report on the possibility to prepare spin-coated thin film in specular optical quality using mixtures of two separate source chalcogenide glass solutions of different compositions ($As_{40}S_{60}$ and $Ge_{20}Sb_5S_{75}$). Thin films with compositions $(As_{40}S_{60})_x(Ge_{20}Sb_5S_{75})_{100-x}$, where x = 0, 25, 50, 75 and 100 were deposited by spin-coating using solution mixtures of $As_{40}S_{60}$ and $Ge_{20}Sb_5S_{75}$ separately dissolved in n-butylamine. Due to the almost linear dependence of thickness and optical parameters on mixtured composition (obtained by changing the source chalcogenide glass solution ratios), the described solution mixing process is suitable for easy and technologically simple preparation of chalcogenide thin films with tailored properties.

CRediT author statement

Jiri Jancalek: Conceptualization, Investigation, Formal analysis, Writing -Original Draft, Visualization.

Stanislav Slang: Investigation, Writing - Review & Editing, Formal analysis, Validation, Methodology.

Michal Kurka: Investigation, Formal analysis, Visualization, Validation.

Karel Palka: Writing - Review & Editing, Validation, Methodology, Visualisation, Resources.

Miroslav Vlcek: Supervision, Funding acquisition, Writing - Review& Editing, Validation.

Acknowledgement

Authors appreciate financial support from project “High-sensitive and low-density materials based on polymeric nanocomposites” – NANOMAT (№ CZ.02.1.01/0.0/0.0/17_048/0007376) and grant LM2018103 from the Ministry of Education, Youth and Sports of the Czech Republic.

References

[1] M. Shpotyuk, A. Kovalkiy, R. Golovchak, O. Shpotyuk, J. Non.-Cryst. Solids 498 (2018) 315-322.
[2] K. Tanaka, M. Mikami, Phys. Status Solidi C 8(9) (2011) 2756-2760.

[3] M. Reinfelde, J. Teteris, R. Grants, Chalcogenide Lett. 17 (2020)19-23.
[4] T. Zhou, Z. Zhu, X. Liu, Z. Liang, X. Wang, Micromachines 9 (2018) 337.
[5] E. Guillevic, X. Zhang, T. Pain, L. Calvez, J.L. Adam, J. Lucas, M. Guilloux-Viry, S. Olliver, G. Gadret, Opt. Mater. 31(11) (2009)1688-1692.
[6] K. Tanaka, K. Shimakawa, Amorphous Chalcogenide Semiconductors and Related Materials, Springer, New York (2011).
[7] J.M.P. Almeida, E.C. Barbano,. C.B. Arnold, L. Misiguti, C.R. Mendonca, Opt. Mater. Express 7 (2017) 93-99.
[8] H. Jain, A. Kovalskiy, M. Vlcek, Chalcogenide Glass Resists for Lithography, Chalcogenide Glasses Woodhead Publishing Limited (2014).
[9] E.A. Sanchez, M. Waldmann, C.B. Arnold, Appl. Opt. 50 (14) (2011)1974-1978.
[10] S. Novak, P. T. Lin,Ch. Li, Ch. Lumdee, J. Hu, A. Agarwal, P.G. Kik, W. Deng, K. Richardson, ACS Appl. Mater. Interfaces 9 (2017) 26990-26995.
[11] G.C. Chern, I. Lauks, J. Appl. Phys. 53 (1982) 6979.
[12] K. Palka, T. Syrovy, S. Schroter, S. Bruckner, M. Rothhardt, M. Vlcek, Opt. Mater. Express 4 (2) (2014) 384-395.
[13] J. Orava, T. Kohoutek, T. Wagner, Deposition techniques for chalcogenide thin films, Chalcogenide glasses, Woodhead Publishing Limited (2014).
[14] G. Bulai, O. Pompilian, S. Gurlui, P. nemec, V. Nazabal, N. Cimpoesu, C. Focsa, Nanomaterials 9 (2019) 676.
[15] A. Nezhdanov, D. Usanov, M. Kudryashov, A. Markelov, V. Trushin, G. De Filpo, A. Mashin, Opt. Mater. 96 (2019) 109292.
[16] L. Strizik, T. Wagner, V. Weissova, J. Oswald, K. Palka, L. Benes, M. Krbal, R. Jambor, C. Koughia, S.O. Kasap, J. Mater. Chem. C 5 (2017) 8489.
[17] K. Palka, S. Slang, J. Jancalek, M. Vlcek, J. Non-Cryst. Solids 517 (2019) 76-82.
[18] H.Khan, P.K. Dwivedi, M. Husain, M Zulfequar, J. Mater. Sci. Electron 29 (2018) 12993-13004.
[19] S. Yakunin, D.N. Dirin, L. Protesescu, M. Sytnyk, S. Tollabimazraehno, M. Humer, F. Hackl, T. Fromherz, M.I. Bodnarchuk, M.V. Kovalenko, W. Heiss, ACS Nano 8 (2014) 12883-12894.
[20] T.Gu, J. Gao, E.E. Ostromov, H. Jeong, F. Wu, R. Fardel, N. Yao, R.D. Priestley, G.D. Scholes, Y.L. Loo, C.B. Arnold, ACS Appl. Mater. Interfaces 9 (2017) 18911-18917.
[21] S. Novak, L. Scarpantonio, J. Novak, M.D. Pre, A. Martucci, J.D. Musgraves, N.D. McClenaghan, K. Richardson, Opt. Mater. Express 3(6) (2013) 729-738.
[22] S.Slang, P. Janicek,K. Palka, L. Loghina, M. Vlcek, Mater. Chem. Phys. 203 (2018) 310-318.
[23] S. Song, J. Dua, C.B. Arnold, Opt. Express 18(6) (2010) 5472-5480.
[24] S. Novak, P.-T. Lin, Ch. Li, N. Borodinov, Z. Han, C. Monmeyran, N. Patel, Q. Du, M. Malinowski, S. Fathpour, Ch. Lumdee, Ch. XU, P. G. Kik, W. Deng, J. Hu, A. Agarwal, I. Luzinov, K. Richardson, J. Vis. Exp. 114 (2016) e54379.
[25] S.Slang, P. Janicek, K. Palka, M. Vlcek, Opt. Mater. Express 9 (11) (2019) 4360-4369.
[26] Z.U. Borisova, Glassy Semiconductors, Plenum Press, New York (1981).
[27] K. Palka, S. Slang, J. Buzek, M. Vlcek, J. Non-Cryst. Solids 447 (2016) 104-109.
[28] S.H. Wemple, M. Didomenico, Phys. Rev B 3 (1971) 1338.
[29] R. Swanepoel, J. Phys. E. Sci. Instrum. 16 (1983) 1214.
[30] L. Loghina, K. Palka, J. Buzek, S. Slang, M. Vlcek, J. Non-Cryst. Solids 430 (2015) 21-24.
[31] K. Palka, J. Jancalek, S. Slang, M. Grinco, M. Vlcek, J. Non-Cryst. Solids 508 (2019) 7-14.
[32] G.C. Chern, I. Lauks, A.R. McGhie, J. Appl. Phys. 54 (1983) 4596-4601.
[33] S. Slang, P. Janicek, K. Palka, M. Vlcek, Opt. Mater. Express 6 (2016) 1973-1985.
[34] M. Waldmann, J.D. Musgraves, K. Richardson, C.B: Arnold, J. Mater. Chem. 22 (2012) 17848-17852.

[35] T. Kohoutek, T. Wagner, M. Frumar, A. Chrissanthopoulos, O. Kostadinova, S.N. Yannopoulos, J. Appl. Phys. 103 (2008) 063511.
[36] N.S. Dutta, C.B. Arnold, RSC. Adv. 8 (2018) 35819-35823.
[37] R. Golovchak, O. Shpotyuk, J.S. Mccloy, B.J. Riley, C.F. Windisch, S.K. Sundaram, A. Kovalskiy, H. Jain, Philos. Mag. 90 (34) (2010) 4489–4501.
[38] A. Stronski, M. Vlcek, A. Sklenar, Semicond. Phys. Quantum Electron. Optoelectron. 3 (3) (2000) 394–399.
[39] A.T. Ward, J. Phys. Chem. 72 (1968) 4133-4139.
[40] S. Slang, K. Palka, L. Loghina, A. Kovalskiy, H. Jain, M. Vlcek J. Non-Cryst. Solids 426 (2015) 125-131.
[41] R. Ston, M. Vlcek, H. Jain, J. Non-Cryst. Solids 326-327 (1) (2003) 220-225.
[42] S. Slang, K. Palka, M. Vlcek, J. Non-Cryst. Solids 471 (2017) 415–420.
[43] S. Slang, K. Palka, H. Jain, M. Vlcek, J. Non-Cryst. Solids 457 (2017) 135–140.
[44] H. Guo, H. Tao, Y. Zhai, S. Mao, X. Zhao, Spectrochim. Acta A Mol. Biomol. Spectrosc. 67 (5) (2007) 1351-1356.
[45] T. Haizheng, Z. Xiujian, J. Chengbin, J. Mol. Struct. 697 (1-3) (2004) 23-27.
[46] J. Tauc, Mater. Res, Bull. 3 (1968) 37-46.
[47] G.C. Chern, I. Lauks, K.H. Norian, Thin Solid Films 123 (1985) 289-296.
[48] J. Novak, S. Novak, M. Dussauze, E. Fargin, F. Adamientz, J.D. Musgraves, K. Richardson, Mater. Res. Bull. 48 (2013) 1250-1255.
[49] G.C. Chern, I. Lauks, J. Appl. Phys. 54 (1983) 2701-2705.